



Synthesis of ZnO nanorods on a silicon substrate via hydrothermal route for optoelectronic applications

Abdulqader D. Faisal¹ · Raid A. Ismail¹ · Wafaa K. Khalef¹ · Evan T. Salim¹

Received: 12 October 2019 / Accepted: 25 March 2020 / Published online: 4 April 2020
© Springer Science+Business Media, LLC, part of Springer Nature 2020

Abstract

In the present work, we have synthesized ZnO nanorods (ZnO NRs) by using hydrothermal technique. The morphological, structural and optical properties of ZnO NRs were investigated using x-ray diffraction (XRD), scanning electron microscope (SEM) and UV–Vis absorption. XRD pattern confirms the deposited film was highly oriented crystalline ZnO NRs along [002] direction. SEM shows the formation of submicron and NRs morphology. The optical absorption studies depict that the optical energy gap of the film was 3.5 eV. The fabricated n-ZnO NRs/p-Si heterojunction photodetector exhibits rectification properties with an ideality factor of 2.2. The highest responsivity and quantum efficiency of the photodetector were nearly 0.27 A/W and 89% at 350 nm, respectively, without using buffer layer.

Keywords ZnO · Nanorods · Hydrothermal · Visible-blind photodetector · Photodetector

1 Introduction

Nanostructured materials have drawn attention due to their superior structural, optical and electrical properties which enable them to be used for many industrial and technological applications. Ultraviolet (UV) and high energy optoelectronic devices, such as UV detectors, laser diodes in the ultraviolet region, and light-emitting diodes, have opened the gate for a wide field of application, for example, high-density information storage, laser printing, optical fiber communication, and others (Salem et al. 2016; Kim et al. 2011; Salavati-Niasari et al. 2008; Babaheydaria et al. 2012; Yousefi et al. 2014). ZnO is a direct and wide energy gap semiconducting material and due to its versatile physical and chemical properties, it used in many industrial applications such as optoelectronics, light sensing, biological, and green energy applications (Fa et al. 2006; Salem et al. 2013; Salim et al. 2016; Sun et al. 2011). Baxter and Aydil (2006) designed a novel DSSC solar cell using ZnO nanomaterials as a wide bandgap n-type semiconductor, Alver et al. (2007) used ZnO films as film transistor, Agnieszka and Tcofil (Agnieszka and Tcofil 2014) employed ZnO in medical application as a plaster material besides many other applications. Hassanpour et al. (2017)

✉ Raid A. Ismail
raidismail@yahoo.com

¹ Applied Science Department, University of Technology, Baghdad, Iraq

used ZnO based nanocomposite in water treatment as methylene blue MB and rhodamine B removal. Goudarzi et al. (2017) utilized ZnO nanoparticles as a photocatalyst for the decolorization of MO under ultraviolet -light irradiation. Various growth methods have been used to prepare ZnO films, such as sputtering, pulsed laser deposition (Salem et al. 2016; Aimsha et al. 2010) ion beam sputtering (Baxter and Aydil 2006) chemical vapour deposition (Chen et al. 2009), sol-gel spin-coating technique (Choi 2010), molecular beam epitaxial (Kim 2009), plasma vapour deposition (Kim et al. 2010), and hydrothermal method (Jeon 2010). It is worth noting that the used method and condition play an important role in controlling the obtained ZnO nanostructures with different morphology, thermal decomposition of $[\text{Zn}(\text{C}_2\text{O}_4)]$ -oleylamine complex has been used to prepare ZnO nanotriangles (Salavati-Niasari et al. 2009a), ZnO nanosphericals were prepared using $[\text{Zn}(\text{salen})]$ thermal decomposition for 90 min at 290 °C in the presence of oleylamine. ZnO nanobundle was synthesized using $[\text{Zn}(\text{salen})]$ thermolysis at 500 °C in the air for 5 h (Salavati-Niasaria et al. 2011). Large quantity of (15–25) nm ZnO nanocrystals was obtained via thermolysis of zinc acetophenato in oleylamine and triphenylphosphine under mild conditions (Salavati-Niasari et al. 2009b). Flowers like ZnO nanostructures were synthesized using $[\text{Zn}(\text{C}_2\text{O}_4)\cdot 2\text{H}_2\text{O}]$ solution with help of microwave-assisted polyol method (Mira et al. 2012). Fiber-like ZnO nanostructures morphologies were obtained using solution free and solid state de-composition of zinc precursor at 400 °C (Soofivand et al. 2013). Hydrothermal can be considered as simple, low-temperature and inexpensive technique to grow single crystal metal oxide nanostructures (Aneesh et al. 2007). It is found to be the most promising method due to the growth of low crystalline deformation such as dislocation density beside that and it is a cost-effective technique compared with other growth techniques (Luo et al. 2010). Besides the last benefit of this method, it is preferred in the production of uniform nanoparticles, especially in the preparation of nanocomposite and nano-hybrid materials. Herein, we report the fabrication and characterization of visible-blind ZnO NRs/Si photo-detector by using a hydrothermal method without using post-annealing and/or buffer layer.

2 Experimental

ZnO nanostructures films were prepared by hydrothermal technique on quartz and single crystal silicon substrates. The silicon substrate used here was mirror-like p-type with an electrical resistivity of (5–10) Ω cm and orientation of (111). In the beginning, the silicon wafer was cut into square pieces with an area of 1 cm² and then cleaned with acetone and ethanol for 30 min.. These substrates were then washed with deionized water (DI) and dried with nitrogen gas. The deposition of nanostructured ZnO was carried out in two steps; in the first step, the seed layer of ZnO nanocrystals was prepared by the drop-casting method. Zinc acetate $[\text{Zn}(\text{CH}_3\text{COO})_2]$ of 10 mM was dissolved in 10 ml of ethanol to form an aqueous solution. The pre-coated silicon substrates with ZnO nanostructured film have been annealed at 350 °C for one hour for the ZnO nanocrystals formation. In the second step, an aqueous growth solution of a 25 mM zinc nitrate $[\text{Zn}(\text{NO}_3)_2\cdot 6\text{H}_2\text{O}]$ and 25 mM hexamethylenetetramine (HMTA) was prepared. Sonication of the solution for 30 min was carried out. Afterward; the pre-coated Si substrates with ZnO NRs film were horizontally immersed in the growth solution and loaded into the oven at 85 °C for 4 h. After that, the substrates were rinsed in deionized water DI water and finally, they dried with nitrogen gas. X-ray diffractometer (XRD-6000, Shimadzu) was employed to investigate the structural properties of ZnO film deposited on the glass substrate. Scanning electron microscope

SEM (T-scan Vega III Czech) was used to investigate the surface morphology of ZnO film. The chemical composition of the prepared film was investigated using energy dispersive x-ray EDX equipped with SEM. The optical absorbance of nanostructured ZnO film was measured by using UV–Vis double beam spectrophotometer (Lambda 750, Perkin Elmer). The morphology and size of ZnO nanorods measurement were determined using high-resolution transmission electron microscope HRTEM (JEOL-2000 EX). Indium thin film and aluminum thick film were deposited, respectively, on ZnO NRs and the silicon substrate to conduct ohmic contacts. Figure 1 shows the architecture of n-ZnO NRs/p-Si photodetector and the sensitive area of the photodetector was around 8 mm².

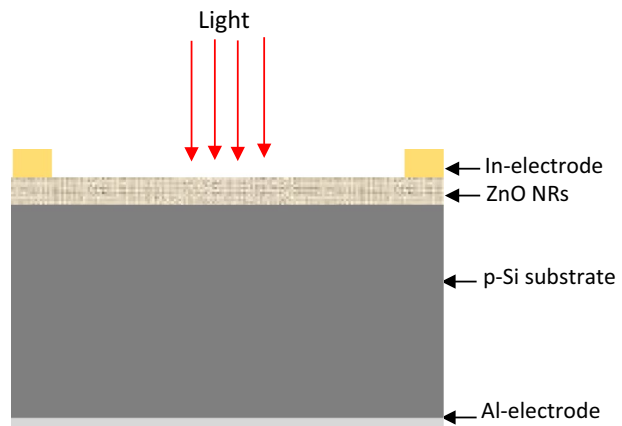
The Current–voltage characteristics under dark and illuminated condition were measured at room temperature using DC power supply, Keithley electrometer and halogen lamp connected with variac to control light intensity. The spectral responsivity of the photodetector was measured in the spectral region of (300–950) nm at 5 V reverse bias voltage by using Jobin Yvon monochromator after power calibration using Sanwa silicon power meter. The spectral responsivity was performed under effect 5 V reverse bias.

3 Results and discussion

Figure 1 illustrates the XRD pattern of ZnO NRs deposited on a silicon substrate. It is seen that five XRD peaks were noticed at $2\theta = 31.8^\circ, 34.6^\circ, 36.3^\circ, 46.6^\circ,$ and 62° corresponding to (100), (002), (101), (102), and (103) planes, respectively.

These peaks are indexed to the polycrystalline ZnO with wurtzite structure according to JCPDs # 01-079-0205 (Jangir et al. 2017). These peaks are close to those of ZnO film prepared by precipitation method (Yousefi et al. 2014). The highest intense peak was observed along the direction [002] indicates a highly oriented c-axis ZnO NRs. No other XRD peaks have been found could be related to impurities or zinc complex indicates the purity of the grown film. The mean crystallite size of ZnO was calculated using Debye–Scherrer equation along (002) plane and found to be approximately 28 nm. The SEM image of ZnO NRs prepared on a silicon substrate is shown in Fig. 2. As shown, the grown film has nanorods morphology with different dimensions.

Fig. 1 Schematic diagram of n-ZnO NRs/p-Si heterojunction photodetector



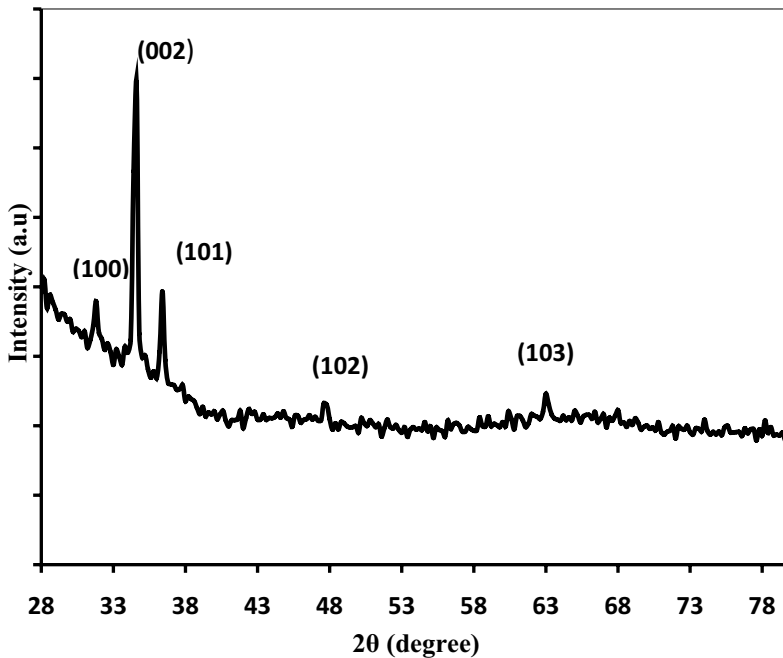


Fig. 2 XRD pattern of ZnO NRs deposited on silicon substrate

The magnified SEM images of Fig. 3 confirmed the presence of submicron and nano-sized rods with different lengths. The nanorods are distributed over the silicon substrate; the average rod diameter was 75 nm and the length of 400 nm. Figure 3 also shows the presence of ZnO nanoparticles with different sizes distributed over the substrate. The EDX spectrum of ZnO NRs depicted in Fig. 4 shows the existence of only the peaks related to Zn and O elements indicates the purity of the prepared ZnO NRs. The atomic molar ratio [Zn]/[O] was determined from EDX analysis and was found to be 0.95 indicates the prepared film is stoichiometric.

Figure 5 shows the HRTEM image of single ZnO NR with selected area electron diffraction (SAED) pattern. As shown, the NRs are growing in the direction of c-axis [0002]. The average diameter of ZnO nanorods measured from TEM image was around 70 nm and the length of 350 nm. The electron diffraction taken on a single ZnO nanoroad confirms the crystallinity structure of ZnO NRs. Figure 6 shows the photographs of ZnO films deposited on the quartz substrates by hydrothermal technique at same condition. As clearly seen in Fig. 6, the deposited films are highly transparent and uniform and no voids or microcracks have been observed on the film surface.

Figure 7a depicts the optical absorption of ZnO NRs grown on the quartz substrate. A broad absorption peak at 355 nm was noticed due to the confinement effect of ZnO NRs (Debanath and Karmakar 2013). After this wavelength, the film absorption decreases up to 470 nm and tends to saturate after 470 nm. The optical energy gap of ZnO NRs was found by extrapolation of the linear part of $(\alpha h\nu)^2$ versus plot to photon energy axis as shown in Fig. 7b according to following relationship

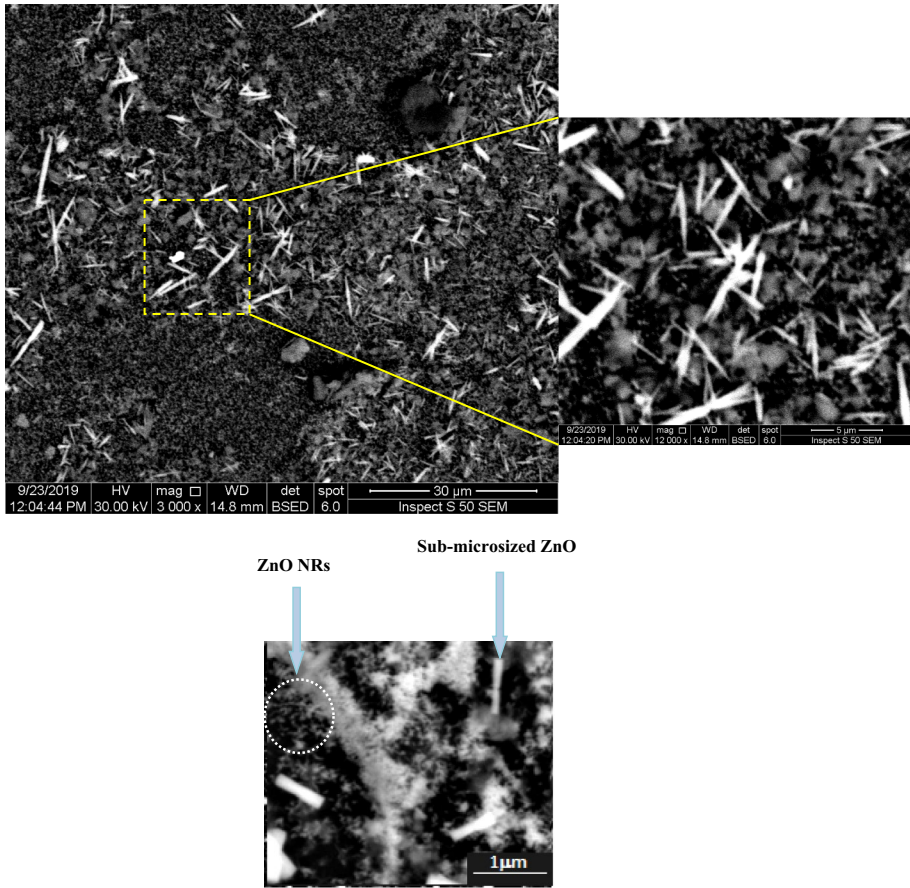


Fig. 3 SEM images of ZnO nanorods deposited on silicon with different magnifications

$$\alpha h\nu = A(h\nu - E_g)^n \tag{1}$$

where A is the constant depends on film material and n is the exponent, and equal to 0.5 for a direct energy gap. As shown in Fig. 7b, the optical band gap of ZnO NRs is 3.5 eV, which is larger than that of the bulk ZnO because of the blue shift comes from the quantum size effect (Ismail et al. 2011).

Figure 8 reveals the variation of electrical resistivity of the ZnO film versus the operating temperature. As shown, the electrical resistivity decreases from 477 to 453 Ωcm as the temperature increases from 303 to 413 K indicates the semiconducting nature of the deposited nanostructured ZnO film. The activation energy E_a of ZnO film was determined from the slope of the linear part of the plot $\ln\rho$ versus the reciprocal of temperature as shown in the inset of Fig. 8 and found to be 14 meV which agree well with reported data for pure ZnO film (Nistor et al. 2016).

Figure 9 displays the room temperature dark I–V characteristics of n-ZnO NRs/p-Si at forward and reverse directions. I–V properties of the photodetector exhibit rectifying properties (diode-like) and the forward current was found to be increased with bias

Fig. 4 EDX spectrum of ZnO nanostructure film

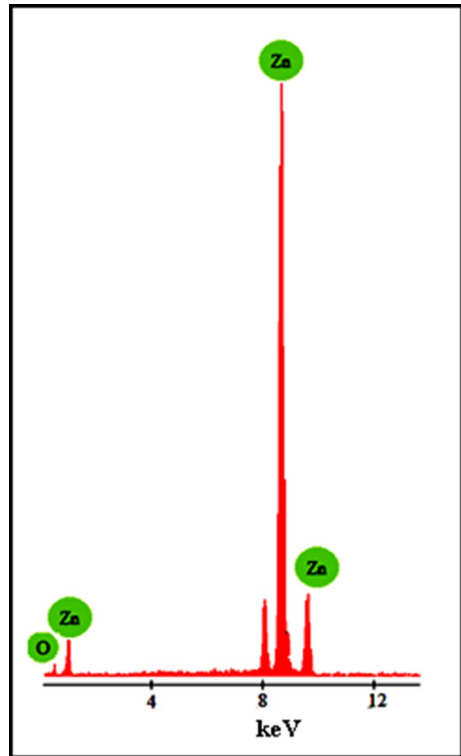


Fig. 5 HRTEM image of single ZnO nanorod. The inset is the electron diffraction of ZnO NRs

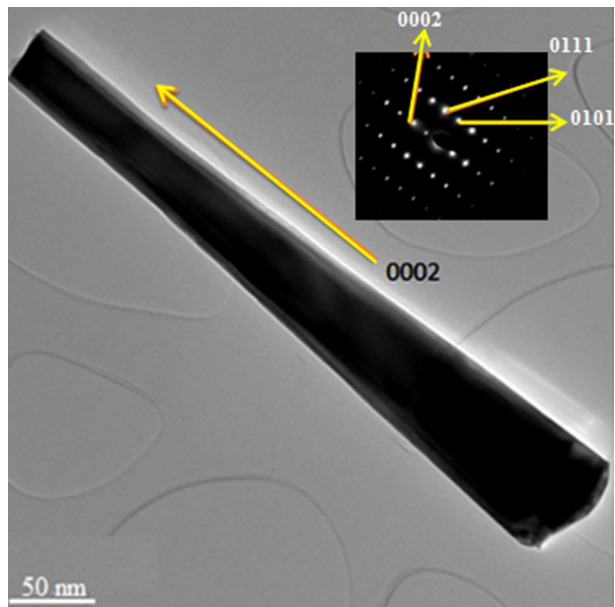


Fig. 6 Photograph of ZnO films deposited on quartz substrate

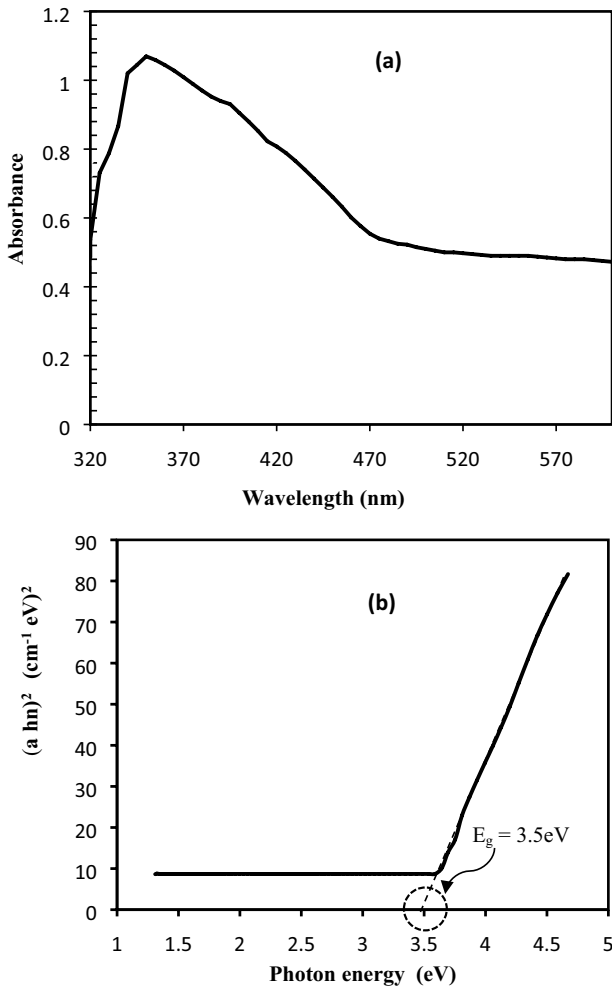
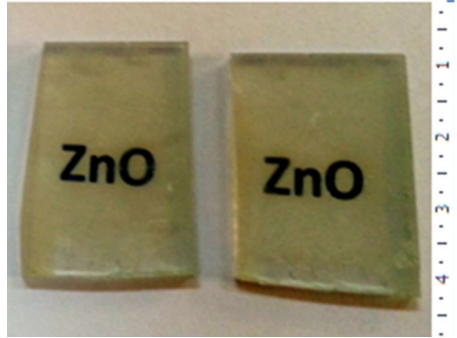


Fig. 7 **a** Optical absorption of nanostructured ZnO, **b** $(\alpha h\nu)^2$ versus photon energy plot

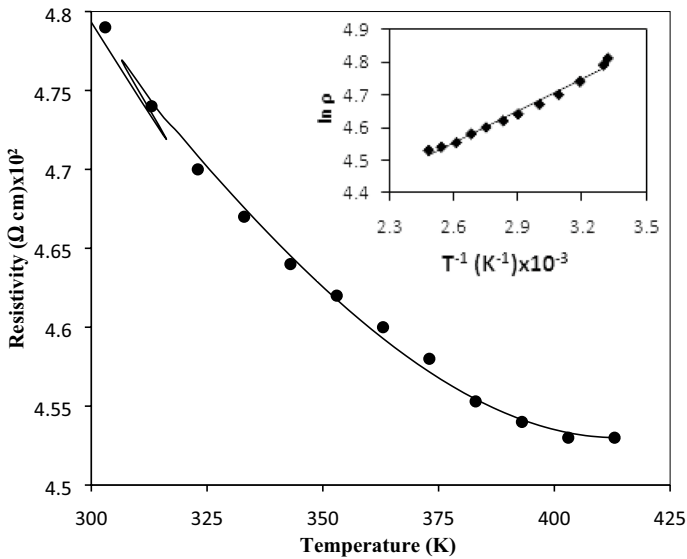


Fig. 8 Variation of resistivity with a temperature of ZnO film. Inset is the $\ln \rho$ versus T^{-1} plot

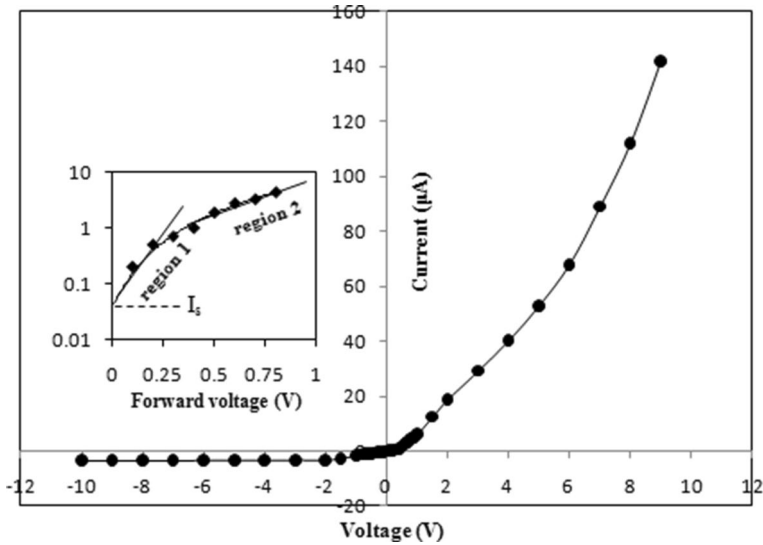


Fig. 9 Dark I–V characteristics of n-ZnO NRs/p-Si heterojunction. Inset is the semi-logarithmic I_f – V_f plot

voltage, while the reverse current was voltage independent. Under forward bias, the current transport at $V_f < 1$ V obeys the ohmic behavior and it increases notably after this voltage and deviates from ohmic behavior confirms the domination of diffusion current. The ideality factor n was determined by plotting $\ln I_f$ versus forward voltage (inset of Fig. 9) and by using the diode equation

$$n = \frac{q}{kT} \left(\frac{\partial v}{\ln \left(\frac{I}{I_s} \right)} \right) \tag{2}$$

where I_s represents the saturation current of the heterojunction which estimated from the extrapolating the linear part (region 1) of the $\ln I_f$ versus V_f plot (inset of Fig. 9) to $V = 0$ point and it founds to be approximately 70 nA. The ideality factor of ZnO/Si heterojunction was found to be 2.2 confirms that the fabricated heterojunction has a low density of structural defects (Ismail et al. 2005, 2006). The obtained ideality factor was comparable to that for ZnO/Si heterojunction prepared by sol–gel technique (Sarkar et al. 2012).

The spectral responsivity R_λ of the photodetector is considered one of the most important figures of merit of the photodetector that describe the photodetector performance (Ismail 2009; Ismail et al. 2017a) and it can be estimated using the following equation

$$R_\lambda = \frac{I_L - I_d}{P} = \frac{I_{ph}}{P} \tag{3}$$

where I_L is the illuminated current, I_{ph} is the photocurrent of the photodetector and P is the power of light at specific wavelength. The responsivity and corresponding quantum efficiency of n-ZnO NRs/p-Si heterojunction photodetector at 5 V bias are shown in Fig. 10. As seen, two response peaks have been observed situated at 350 nm (UV region) and 840 nm (NIR) which are belonging to the absorption edge of ZnO NRs and the silicon substrate, respectively (Ismail et al. 2017b). The responsivity of the photodetector at 350 nm was 0.27 A/W corresponding to quantum efficiency of 89%, while the responsivity and quantum efficiency of the photodetector at 840 nm were 0.09A/W and 28%, respectively. The maximum responsivity of the photodetector prepared by this technique is comparable to those reported for ZnO/Si photodetector prepared by other methods (Chen and Pan 2008; Hazra et al. 2014; Ismail et al. 2014). The responsivity of the photodetector at the visible region is flat and low (visible-blind photodetector). The specific detectivity D^* and

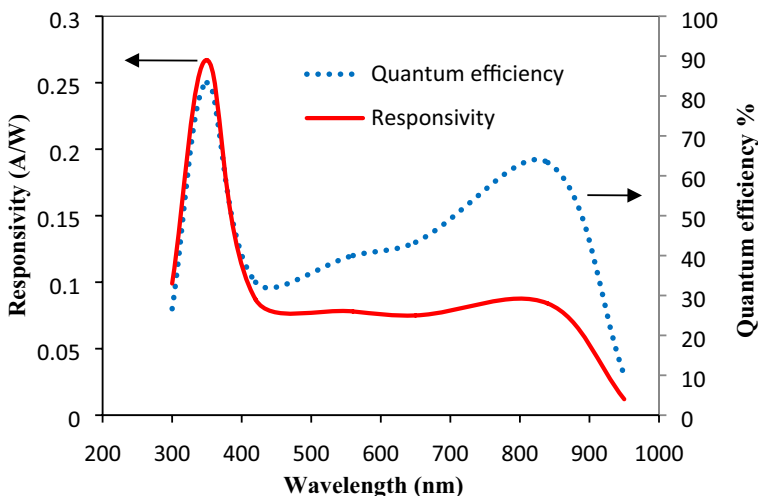


Fig. 10 Responsivity and quantum efficiency of ZnO NRs/Si photodetector at 5 V bias

Table 1 Comparison of figures of merit of ZnO/Si photodetector prepared by different techniques

Technique	Responsivity (A/W)	EQE %	D* (Jones)	References
Hydrothermal	0.27 (at 350 nm)	89	3.4×10^{11}	Present work
RF magnetron	7.1 (at 442 nm)	–	7.1×10^9	Wang (2014)
Laser deposition	21.5 (at 365)	73.1×10^2	1.26×10^{12}	Flemban et al. (2017)

noise equivalent power NEP of the ZnO/Si heterojunction photodetector were found from responsivity and dark I–V data at 5 V bias and found to be 3.4×10^{11} Jones and 2.9 pW, respectively.

Table 1 shows the obtained values of figures of merit of ZnO/Si photodetector fabricated by hydrothermal method compared to some ZnO/Si heterojunctions prepared by other techniques. As can be seen, the parameters of the photodetector are depended strongly on the deposition method.

4 Conclusion

In summary, we have fabricated UV-sensitive ZnO NRs/Si heterojunction photodetectors by using simple hydrothermal route without using a buffer layer. The morphological, structural, optical, and electrical properties of nanostructured ZnO film have been studied. XRD data confirm the formation of polycrystalline ZnO with wurtzite structure and the grains are highly oriented along [002] direction. The optical absorption of ZnO film shows a broad peak at 350 nm and the direct optical energy gap of ZnO film was 3.5 eV. SEM investigation reveals that the deposited film has nanorods morphology with different dimensions. EDX result confirms that the deposited film is stoichiometric. TEM and electron diffraction investigations confirmed formation of high quality ZnO nanorods with an average size of 70 nm and the crystal direction was around [0002]. The ideality factor of the ZnO/Si photodetector was 2.2. The maximum responsivity of the ZnO NRs/Si photodetector without post-annealing was 0.27A/W at in the UV region. The specific detectivity of the photodetector was 3.4×10^{11} Jones and the external quantum efficiency was 89% at 350 nm. The photodetector parameters, namely responsivity, quantum efficiency and detectivity were compared with those for photodetector prepared by others methods. The technique used here is cost-effective, simple, reliable, and promising for preparation of high photosensitivity ZnO NRs/Si visible-blind heterojunction photodetector.

References

- Agnieszka, K.R., Tcofil, J.: Zinc oxide—from synthesis to application: a review. *Materials* **7**, 2833–2881 (2014)
- Aimsha, R.S., Manoj, R., Aneesh, P.M., Jayaraj, M.K.: Violet luminescence from ZnO nanorods grown by room temperature pulsed laser deposition. *Curr Appl. Phys.* **10**, 693–697 (2010)
- Alver, U., Kılınc, T., Bacaksız, E., Küçükömeroğlu, T., Nezir, S., Mutlu, İ.H., Aslan, F.: Synthesis and characterization of spray pyrolysis zinc oxide microrods. *Thin Solid Films* **515**, 3448–3451 (2007)
- Aneesh, P.M., Vanaja, K.A., Jayaraj, M.K.: Synthesis of ZnO nanoparticles by hydrothermal method" *Nanophotonic Materials IV*, edited by Zeno Gaburro, Stefano Cabrini. *Proc. SPIE* **6639**, 66390J (2007)

- Babaheydari, A.K., Salavati-Niasarib, M., Khansari, A.: Solvent-less synthesis of zinc oxide nanostructures from Zn(salen) as precursor and their optical properties. *Particuology* **10**, 759–764 (2012)
- Baxter, J.B., Aydil, E.S.: Dye-sensitized solar cells based on semiconductor morphologies with ZnO nanowires. *Solar Energy Mater. Solar Cells*. **90**, 607–622 (2006)
- Chen, L., Pan, C.: P-ZnO/n-Si photodiodes prepared by ultrasonic spraying pyrolysis method. *Open Crystallogr. J.* **1**, 10–13 (2008)
- Chen, J.Y., Pan, C.J., Taso, F.C., Kuo, C.H., Chi, G.C., Pong, B.J., Chang, C.Y., Norton, D.P., Pearton, S.J.: Characterization of ZnO nanowires grown on Si (100) with and without Au catalyst. *Vacuum* **83**(7), 1076–1079 (2009)
- Choi, H.Y., et al.: Effects of growth temperature of MBE-seed layers on the structural and optical properties of ZnO thin films prepared by using the sol-gel method. *J. Korean Phys. Soc.* **56**, 1514–1518 (2010)
- Debanath, M., Karmakar, S.: Study of blue shift of optical band gap in zinc oxide (ZnO) nanoparticles prepared by low-temperature wet chemical method. *Mater. Lett.* **111**, 116–119 (2013)
- Fa, S., Feitknecht, L., Schluchter, R., Kroll, U., Vallat-Sauvainand, E., Shah, A.: Rough ZnO layers by LP-CVD process and their effect in improving performances of amorphous and microcrystalline silicon solar cells. *Sol. Energy Mater. Sol. Cells* **90**(18–19), 2960–2967 (2006)
- Flemban, T., et al.: A photodetector based on p-Si/n-ZnO nanotube heterojunctions with high ultraviolet responsivity. *ACS Appl. Mater. Interfaces* **9**, 37120–37127 (2017)
- Goudarzi, M., Mousavi-Kamazani, M., Salavati-Niasari, M.: Zinc oxide nanoparticles: solvent-free synthesis, characterization and application as heterogeneous nanocatalyst for photo degradation of dye from aqueous phase. *J. Mater. Sci. Mater. Electron.* **28**, 8423–8428 (2017)
- Hassanpour, M., Safardoust-Hojaghan, H., Salavati-Niasari, M.: Degradation of methylene blue and Rhodamine B as water pollutants via green synthesized Co₃O₄/ZnO nanocomposite. *J. Mol. Liq.* **229**, 293–299 (2017)
- Hazra, P., Singh, S.K., Jit, S.: Ultraviolet Photodetection Properties of ZnO/Si heterojunction diodes fabricated by ALD technique without using a buffer Layer. *J. Semicond. Technol. Sci.* **14**, 117–123 (2014)
- Ismail, R.: Characteristics of p-Cu₂O/n-Si heterojunction photodiode made by rapid thermal oxidation. *J. Semicond. Technol. Sci.* **9**, 51–54 (2009)
- Ismail, R.A., Abdulrazaq, O.A., Yahya, K.: Preparation and characterization of In₂O₃ thin films for optoelectronic applications. *Surf. Rev. Lett.* **12**, 515–518 (2005)
- Ismail, R., Raouf, D.N., Raouf, D.F.: High efficiency In₂O₃/c-Si heterojunction solar cells produced by rapid thermal oxidation. *J. Optoelectron. Adv. Mater.* **8**, 1443–1446 (2006)
- Ismail, R., Ali, A., Ismail, M., Hassoun, K.: Preparation and characterization of colloidal ZnO nanoparticles using nanosecond laser ablation in water. *Appl. Nanosci.* **1**, 45–49 (2011)
- Ismail, R.A., Al-Jawad, S.M., Hussein, N.: Preparation of n-ZnO/p-Si solar cells by oxidation of zinc nanoparticles: effect of oxidation temperature on the photovoltaic properties. *Appl. Phys. A* **117**, 1979–1984 (2014)
- Ismail, R., Khashan, K., Mahdi, R.: Characterization of high photosensitivity nanostructured 4H-SiC/p-Si heterostructure prepared by laser ablation of silicon in ethanol. *Mater. Sci. Semicond. Process.* **68**, 252–261 (2017a)
- Ismail, R.A., Alwan, A.M., Ahmed, A.S.: Preparation and characteristics study of nano-porous silicon UV photodetector. *Appl. Nanosci.* **7**, 9–15 (2017b)
- Jangir, L., Kumari, Y., Kumar, A., Kumar, M., Awasthi, K.: Investigation of luminescence and structural properties of ZnO nanoparticles, synthesized with different precursors. *Mater. Chem. Front.* **1**, 1413–1421 (2017)
- Jeon, S.M., et al.: Fabrication of porous ZnO nanorods with nano-sized pores and their properties. *J. Korean Phys. Soc.* **57**, 1477–1481 (2010)
- Kim, M.S., et al.: Improvement in crystallinity and optical properties of ZnO epitaxial layers by thermal annealed ZnO buffer layers with oxygen plasma. *J. Crystal Growth* **311**, 3568–3572 (2009)
- Kim, A.R., Lee, J.-Y., Jang, B.R., Kim, H.S., Park, H.K., Cho, Y.J., Jang, N.W.: Effect of Post Annealing of ZnO Buffer Layer on the Properties of Hydrothermally Grown ZnO Nanorods. *Jpn. J. Appl. Phys.* **49**, 06GH10–16 (2010)
- Kim, M., Yim, K., Cho, M., Leem, J.-Y.: Post-annealing effects on the structural and the optical properties of ZnO thin films grown by using the hydrothermal method. *J. Korean Phys. Soc.* **58**, 515–519 (2011)
- Luo, H., Wei, M., Wei, K.: Synthesis of Nb₂O₅ nanosheets and its electrochemical measurements. *Mater. Chem. Phys.* **120**, 6–9 (2010)
- Mira, N., Salavati-Niasaria, M., Davarc, F.: Preparation of ZnO nanoflowers and Zn glycerolate nanoparticles using inorganic precursors via a convenient route and application in dye sensitized solar cells. *Chem. Eng. J.* **181–182**, 779–789 (2012)

- Nistor, M., Mihut, L., Millon, E., Cachoncinlle, C., Hebert, C., Perriere, J.: Tailored electric and optical properties of Nd-doped ZnO: from transparent conducting oxide to photon down-shifting thin film. *RSC Adv.* **6**, 41465–41472 (2016)
- Salavati-Niasari, M., Davar, F., Mazaheri, M.: Preparation of ZnO nanoparticles from [bis(acetylacetonato) zinc(II)]-oleylamine complex by thermal decomposition. *Mater. Lett.* **62**, 1890–1892 (2008)
- Salavati-Niasari, M., Mirb, N., Davar, F.: ZnO nanotriangles: synthesis, characterization and optical properties. *J. Alloy. Compd.* **476**, 908–912 (2009a)
- Salavati-Niasari, M., Davar, F., Fereshteha, Z.: Synthesis and characterization of ZnO nanocrystals from thermolysis of new precursor. *Chem. Eng. J.* **146**, 498–502 (2009b)
- Salavati-Niasaria, M., Davara, F., Khansaric, A.: Nanosphericals and nanobundles of ZnO: Synthesis and characterization. *J. Alloys Compd.* **509**, 61–65 (2011)
- Salem, E.T., Fakhry, M.A., Hassen, H.: Metal oxide Nanoparticles suspension for optoelectronic devises fabrication. *Int. J. Nanoelectron. Mater.* **6**, 121–128 (2013)
- Salem, E.T., Ismail, R.A., Fakhry, M.A., Yusof, Y.: Reactive PLD of ZnO thin film for optoelectronic application. *Int. J. Nanoelectron. Mater.* **9**, 111–122 (2016)
- Salim, E.T., Fakhri, M.A., Hassan, H., Salim, Z.T.: Physicochemical properties of ZnO nanoparticles prepared using low energy low repetition rate laser system. *Sci. Int. (Lahore)* **28**, 4501–4506 (2016)
- Sarkar, S., Patra, S., Bera, S., Paul, G.K., Ghosh, R.: Rectifying properties of sol–gel synthesized Al:ZnO/Si (N–n) thin film heterojunctions. *Phys. E* **46**, 1–5 (2012)
- Soofivand, F., Salavati-Niasari, M., Mohandes, F.: Novel precursor-assisted synthesis and characterization of zinc oxide nanoparticles/nanofibers. *Mater. Lett.* **98**, 55–58 (2013)
- Sun, K., Wei, W., Ding, Y., Jing, Y., Wang, Z.L., Wang, D.: Crystalline ZnO thin film by hydrothermal growth. *Chem. Commun.* **47**, 7776–7778 (2011)
- Wang, Z.: Optimizing performance of silicon-based p-n junction photodetectors by the piezo-phototronic effect. *ACS Nano* **8**, 12866–12873 (2014)
- Yousefi, M., Noori, E., Ghanbari, D., Salavati-Niasari, M.: A facile room temperature synthesis of zinc oxide nanostructure and its influence on the flame retardancy of poly vinyl alcoholtahereh gholami. *J Clust Sci* **25**, 397–408 (2014)

Publisher's Note Springer Nature remains neutral with regard to jurisdictional claims in published maps and institutional affiliations.